Supporting Information

C=C bond enables difluorideboron *β*-diketonate derivative with high contrast mechanoresponsive luminescence for reversible writing and information encryption

Yan Xia[1], Geng Li[1], Xiangkai Yin[1], Jie Li[1*], Juemin Zhao[1], Kunpeng Guo[1*], Yaxing Tang[1], Hua Wang[1,2*]

[1] *Ministry of Education Key Laboratory of Interface Science and Engineering in Advanced Materials, College of Materials Science and Engineering*

Taiyuan University of Technology

Taiyuan, 030024, China

[2] *College of Textile Engineering*

Taiyuan University of Technology

Jin Zhong, 030600, China

E-mail: lijie01@tyut.edu.cn; guokunpeng@tyut.edu.cn; wanghua001@tyut.edu.cn

Table of contents

1. Experimental Section

1.1 Materials and Characterization

Unless otherwise specified, all reagents and solvents were purchased from Energy Chemical Co., Ltd. and used without purification. All reactions were carried out under N_2 atmosphere and anhydrous conditions unless noted otherwise. ^{1}H NMR and ^{13}C NMR spectra NMR spectra were recorded on a Bruker NMR 600 spectrometer. Mass spectrometric measurements were performed on a Ultraflex MALDI-TOF/TOF mass spectrometer, with α-cynao-4-hydroxycinnamic acid (CHCA) as the matrix. Elemental analysis was run on a Vario EL III Elemental Analyzer. UV–vis absorption spectra were performed on a HITACHI U-3900 Spectrometer. Photoluminescence (PL) spectra were recorded on a HITACHI F-4700 spectrometer. The absolute fluorescence quantum yields of solution (10^{-5} M) and powder were measured on Edinburgh Instrument FLS980 spectrometer using an integrating sphere. The transient photoluminescence decay profiles of the solids were recorded using an Edinburgh Instrument FLS980 spectrometer equipped with an EPL-375 ps pulsed diode laser. Powder X-ray diffraction measurements were carried out on a Bruker X-ray diffractometer. Single-crystal X-ray diffraction data was collected on an Agilent Super Nova (Dual, Cu at zero, Eos) diffractometer. Using Olex2, the structure was solved with the ShelXS structure solution program using Direct Methods and refined with the ShelXL refinement package using Least Squares minimisation. Differential scanning calorimetry (DSC) measurements were carried out on a NETZSCH DSC204 instrument at a heating rate of 10 K min^{-1} under nitrogen atmosphere. Fourier transform infrared (FT-IR) spectra measurements were used VERTEX 70v instrument.

1.2 Theoretical Calculation

The geometries as well as the molecular orbital distributions were optimized by DFT/B3LYP

calculation on the 6-31G(d) basis, and the electronic excited states were calculated by TD-DFT/B3LYP calculation on 6-31+G(d, p) basis. Multiwfn 3.8 software package and VMD 1.9.3 were used to perform the charge distribution. [S1-S3]

1.3 Synthesis

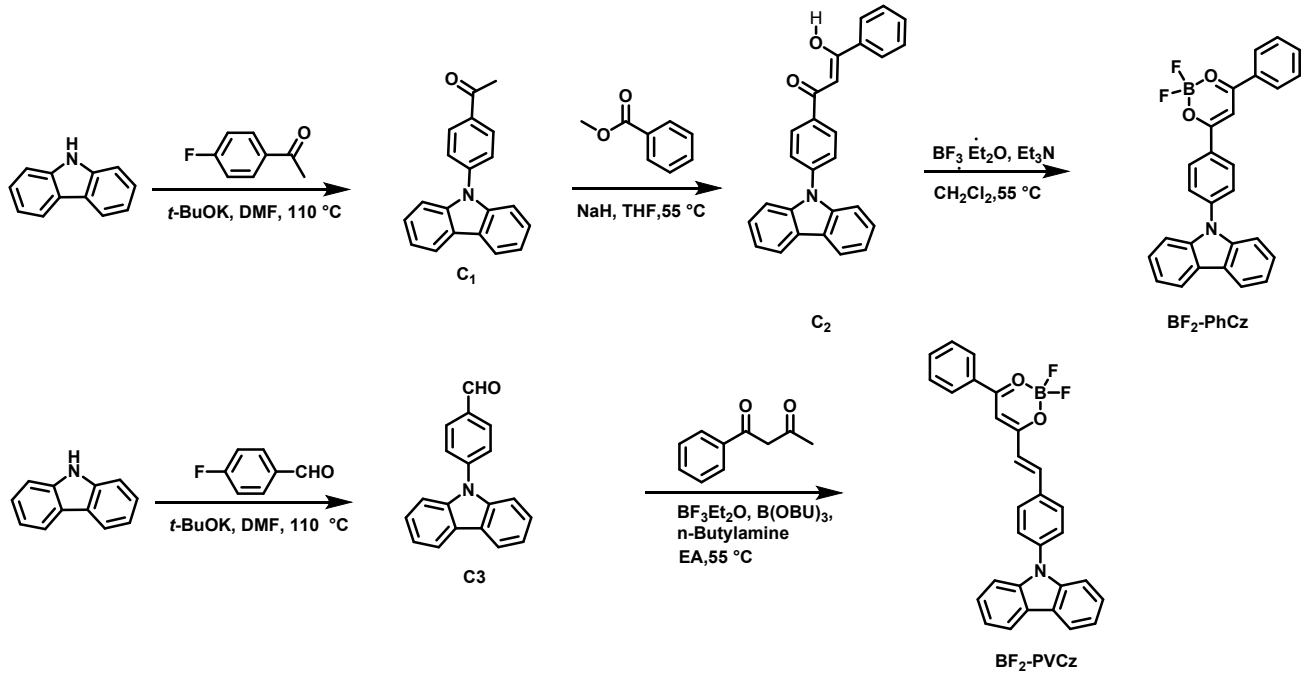

Scheme S1. Synthesis route to compounds **BF_2-PhCz** and **BF_2-PVCz**.

The synthesis of ***C_1***

A mixture of carbazole (1.67 g,10 mmol), 4-fluorophenone (1.38 g,10 mmol) and potassium *tert*-butoxide (0.56 g, 5 mmol) were added to N, N-dimethylformamide (DMF) (30 mL) solution. The mixture was heated to 110 °C and stirred for 24 hours. After cooling to room temperature, the products were poured into water and then filtered. The residue was washed with deionized water, saturated NaCl solution and dissolved in CH_2Cl_2. The organic phase was dried over $MgSO_4$, filtered and concentrated under vacuum. The crude product was purified by column chromatography (petroleum ether: ethyl acetate = 12:1 v/v) to obtain **C_1** as white solid (2.28 g, 8 mmol) with a yield of 80%. ^{1}H NMR (600 MHz, $CDCl_3$) δ 8.14 (d, J = 7.26 Hz, 2H), 7.97 (d, J = 7.86 Hz, 2H), 7.65 (m, 2H), 7.58 (d, J = 8.16

Hz, 2H), 7.32 (m, 4H), 2.56 (s, 3H). ^{13}C NMR (151 MHz, $CDCl_3$) δ 196.83, 140.87, 139.92, 135.98, 129.74, 126.24, 125.08, 123.32, 120.93, 120.26, 110.55, 26.38. MS (MALDI-TOF, m/z): $[M]^+$ calcd for 285.12, found 285.13.

The synthesis of ***C_2***

Compound **C_1** (2.85 g, 10 mmol) and methyl benzoate (1.63 g, 12 mmol) were dissolved in 30 mL THF. Then NaH (0.12 g, 5 mmol) was added, and the mixture was stirred at 60 °C for 20 hours. After cooling to room temperature, the products were poured into water (200 mL). The organic phase was extracted with CH_2Cl_2, washed with deionized water and saturated NaCl solution successively, and dried over anhydrous $MgSO_4$. The organic solvent was evaporated under reduced pressure, and then the crude product was purified by column chromatography (petroleum ether: ethyl acetate = 20:1 v/v) to obtain **C_2** as white solid (1.75 g, 4.5 mmol) with a yield of 45%. ^{1}H NMR (600 MHz, $CDCl_3$) δ 8.24 (d, J = 8.60 Hz, 2H), 8.15 (d, J = 6.78 Hz, 2H), 8.04 (d, J = 7.38 Hz, 2H), 7.74 (d, J = 8.64 Hz, 2H), 7.59 (t, J = 7.35 Hz, 1H), 7.51 (m, 4H), 7.44 (t, J = 7.05 Hz, 2H), 7.33 (t, J = 7.44 Hz, 2H), 6.94 (s, 1H). ^{13}C NMR (150 MHz, $CDCl_3$) δ 185.84, 185.07, 140.87, 140.56, 134.44, 134.01, 131.36, 129.48, 128.16, 127.43, 126.24, 124.92, 123.32, 120.93, 120.26, 110.55, 94.18. MS (MALDI-TOF, m/z): $[M]^+$ calcd for 389.45，found 389.23。

The synthesis of ***BF_2-PhCz***

Compound **C_2** (389 mg, 1 mmol) was dissolved in CH_2Cl_2 (20 mL) and stirred at room temperature, then boron(III) fluoride ethylether complex ($BF_3{\cdot}Et_2O$) (213 mg, 1.50 mmol) and two drops of piperidine were added to the mixture. The mixture was stirred at room temperature for 5 h. The organic phase was extracted with CH_2Cl_2, washed with deionized water and saturated NaCl solution successively, and dried over anhydrous $MgSO_4$. The organic solvent was evaporated under

reduced pressure, and the crude product was purified by column chromatography (petroleum ether: ethyl acetate 4:1 v/v) to obtain orange-yellow solid product **BF_2-PhCz** (175 mg, 0.4 mmol) with a yield of 40%. ^{1}H NMR (600 MHz, $CDCl_3$) δ 8.41 (d, J = 8.70 Hz, 2H), 8.20 (dd, J = 8.55, 1.23 Hz, 2H), 8.15 (d, J = 6.78 Hz, 2H), 7.84 (d, J = 8.64 Hz, 2H), 7.73 (t, J = 6.78 Hz, 1H), 7.59 (t, J = 7.92 Hz, 2H), 7.54 (d, J = 8.28 Hz, 2H), 7.46 (t, J = 7.74 Hz, 2H), 7.35 (t, J = 7.44 Hz, 2H), 7.27 (s, 1H). ^{13}C NMR (151 MHz, $CDCl_3$) δ 181.12, 177.75, 140.87, 140.17, 139.53, 138.19, 131.40, 131.25, 128.02, 126.24, 125.05, 124.60, 123.34, 120.93, 120.26, 110.55, 99.78. MS (MALDI-TOF, m/z): $[M]^+$calcd 437.14，found 437.12.

The synthesis of ***C_3***

Compound carbazole (1.67 g, 10 mmol) was dissolved in N, N-dimethylformamide (DMF, 30 mL) and stirred at room temperature. Then 4-fluorobenzaldehyde (1.24 g, 10 mmol) and potassium *tert*-butoxide (0.56 g, 5 mmol) were added to the mixture. The mixture was heated to 110 °C and stirred for 24 hours. After cooling to room temperature, the solution was poured into water and then filtered. The residue was washed with deionized water and saturated NaCl solution for three times, dissolved in CH_2Cl_2, and dried over anhydrous $MgSO_4$. The organic solvent was evaporated under reduced pressure, and then the crude product was purified by column chromatography (petroleum ether: ethyl acetate = 10:1 v/v) to obtain **C_3** as white solid (2.71 g, 7.5 mmol) with a yield of 75%. ^{1}H NMR (600 MHz, $CDCl_3$) δ 9.93 (s, 1H), 8.14 (d, J = 8.76 Hz, 2H), 7.95 (d, J = 7.80 Hz, 2H), 7.70 (dd, J = 7.80, 1.62 Hz, 2H), 7.65 (m, 2H), 7.31 (m, 4H). ^{13}C NMR (151 MHz, $CDCl_3$) δ 190.57, 140.93, 140.27, 131.78, 131.09, 126.24, 123.32, 122.26, 120.93, 120.26, 110.55. MS (MALDI-TOF, m/z): $[M]^+$calcd 437.14, found 437.12.

The synthesis of ***BF_2-PVCz***

Compound 1-phenyl-1, 3-butanedione (322 mg, 1 mmol) and boron trifluoride diethyl ether (142 mg, 1 mmol) were added to the ethyl acetate (10 mL) solution, then the mixture was heated to 55 °C and stirred for 30 min to obtain system A. System B was obtained by mixing **C_3** (271 mg,1 mmol) and tripropyl borate (56 mg, 0.3 mmol). The mixture of System A and B were continued stirring for 30 min, then *n*-butylamine (6 mg, 0.08 mmol) was added to the mixture at 55 °C. The reaction was quenched and cooled to room temperature after 15 min. The products were poured into water and then filtered. The residue was washed with deionized water and saturated NaCl solution for three times, dissolved in CH_2Cl_2, and dried over anhydrous $MgSO_4$. The organic solvent was evaporated under reduced pressure and the crude products were obtained by column chromatography (petroleum ether: ethyl acetate = 4:1 v/v) to obtain orange-yellow solid product **BF_2-PVCz** (225 mg, 0.6 mmol) with a yield of 60%. ^{1}H NMR (600 MHz, $CDCl_3$) δ 8.21 (d, J = 15.60 Hz, 1H), 8.14 (m, 4H), 7.88 (d, J = 8.30 Hz, 2H), 7.70 (m, 3H), 7.56 (t, J = 8.64 Hz, 2H), 7.51 (d, J = 7.32 Hz, 2H), 7.44 (m, 2H), 7.33 (t, J = 8.01 Hz, 2H), 6.90 (d, J = 15.60 Hz, 1H), 6.71 (s, 1H). ^{13}C NMR (151 MHz, $CDCl_3$) δ 186.28, 184.66, 147.33, 142.83, 138.23, 135.04, 133.64, 132.91, 132.15, 131.87, 129.54, 129.32, 127.18, 124.06, 123.48, 112.72, 102.88, 96.34, 2.84. MS (MALDI-TOF, m/z): $[M]^+$calcd for 463.29, found 463.14.

2. Theoretical Calculation

For both molecules, the highest occupied molecular orbitals (HOMOs) were mostly distributed on the carbazole and π-bridge units, and the lowest unoccupied molecular orbitals (LUMOs) were distributed in boron difluoride *β*-diketone segment and the π-bridge units. The calculated HOMO energies were -5.67 and -5.60 eV, and the LUMO energies were calculated to be -2.74 and -2.85 eV for **BF_2-PhCz** and **BF_2-PVCz**, respectively. The extension of π-bridge reduced the LUMO level and band gap, which would contribute to redshift of luminescence.

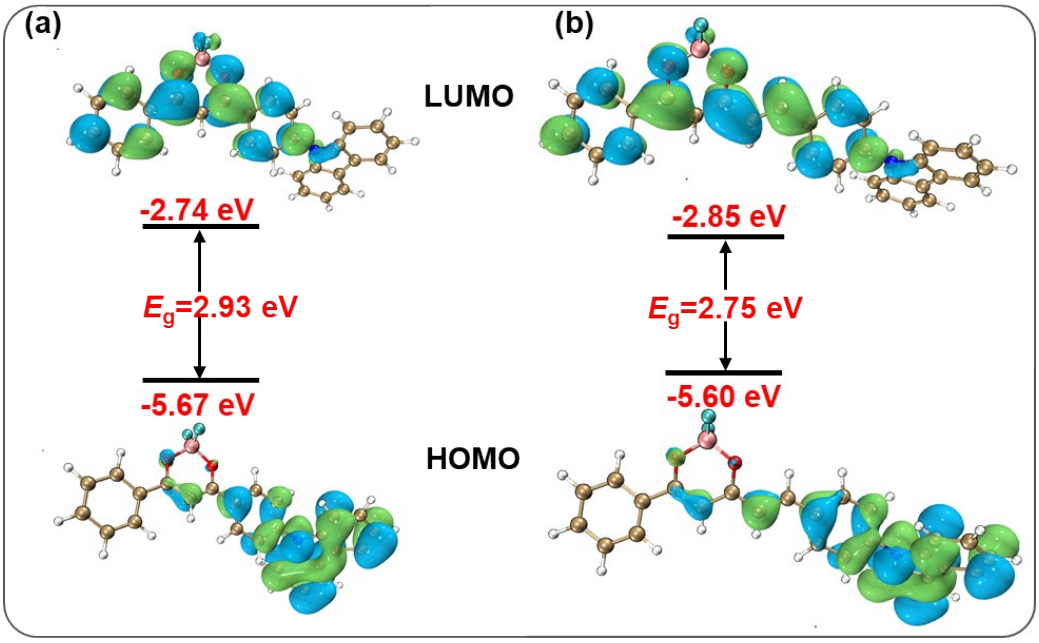

Fig. S1 The spatial distribution of HOMO and LUMO of molecule (a) **BF_2-PhCz** and (b) **BF_2-PVCz**.

Transition dipole moment (TDM) of the compounds were calculated, and the results were shown in Fig. S2. The value of oscillator strength (*f*) is the sum of squares of the singlet excited dipole moments in all directions ($f = x^2+y^2+z^2$), which was proportional to the TDM of the excited state. A larger *f* means higher PLQY.

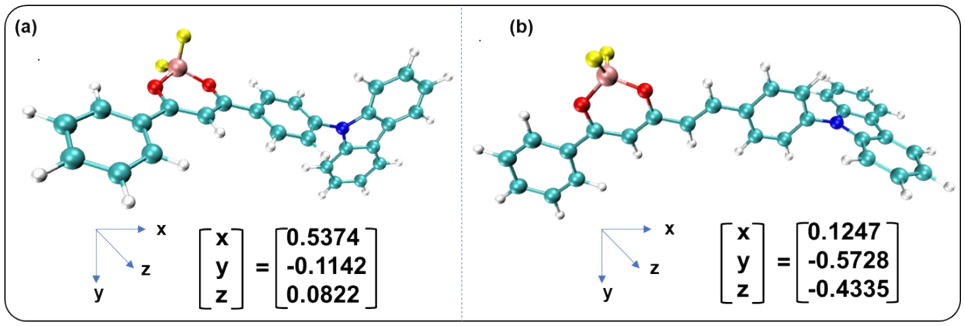

Fig. S2 Transition dipole moment of molecules (a) **BF_2-PhCz** and (b) **BF_2-PVCz** in front view.

3. Photophysical Properties

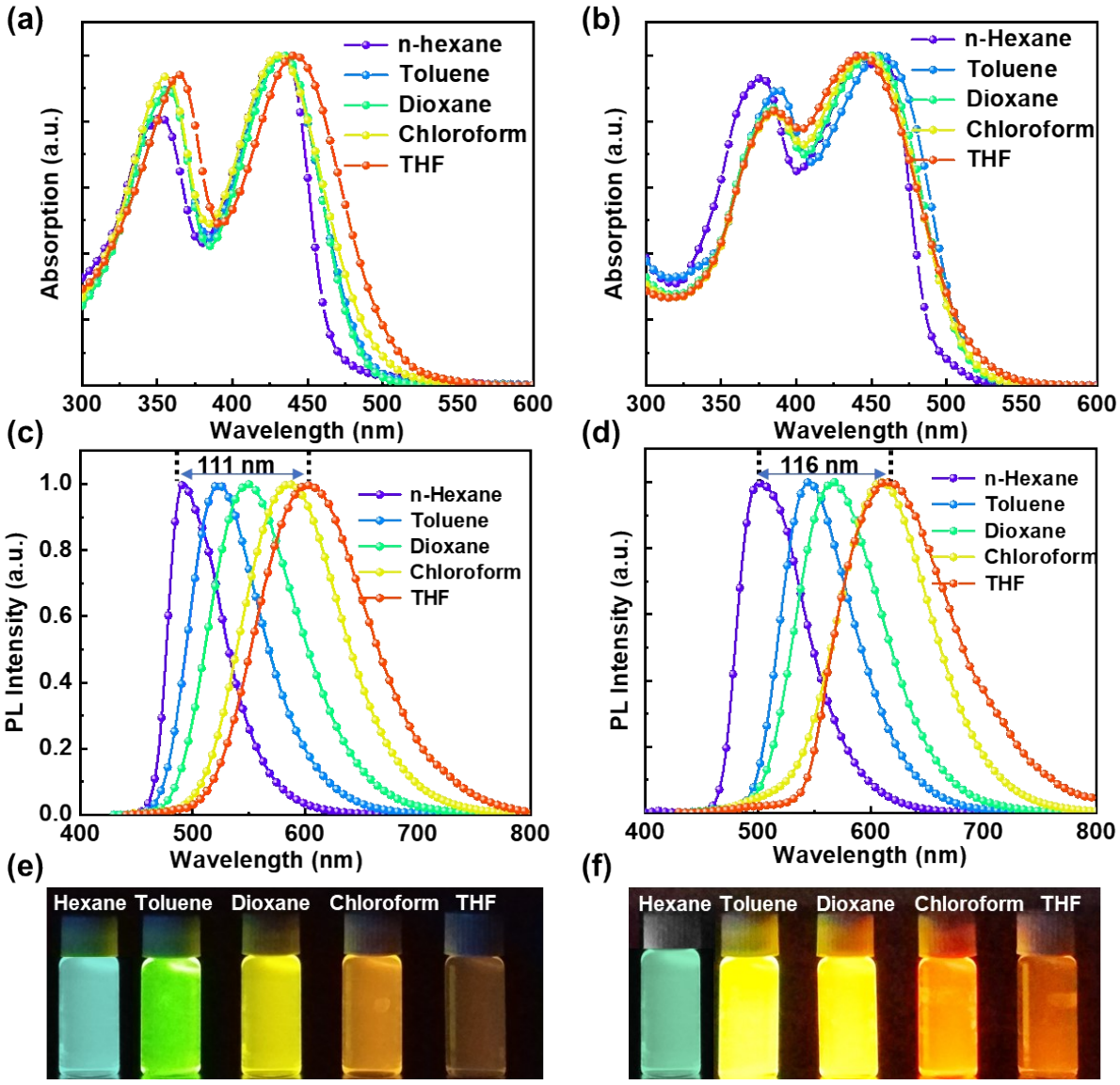

Figure S3. UV-vis absorption spectra of (a) **BF_2-PhCz** and (b) **BF_2-PVCz** in various solvents (10^{-5} M). PL spectra of (c) **BF_2-PhCz** and (d) **BF_2-PVCz** in various solvents (10^{-5} M). Fluorescence photographs of (e) **BF_2-PhCz** and (f) **BF_2-PVCz** in various solvents under irradiation at 365 nm.

As shown in Fig. S4a and S4b, due to the Rayleigh scattering, the absorption bands were dramatically broadened and red-shifted after the water content was above 70% because of the aggregation of molecules. The variation trend of PL intensity and wavelength with the elevated water fractions of **BF_2-PhCz** and **BF_2-PVCz** were depicted in Fig. S4c and S4d, respectively.

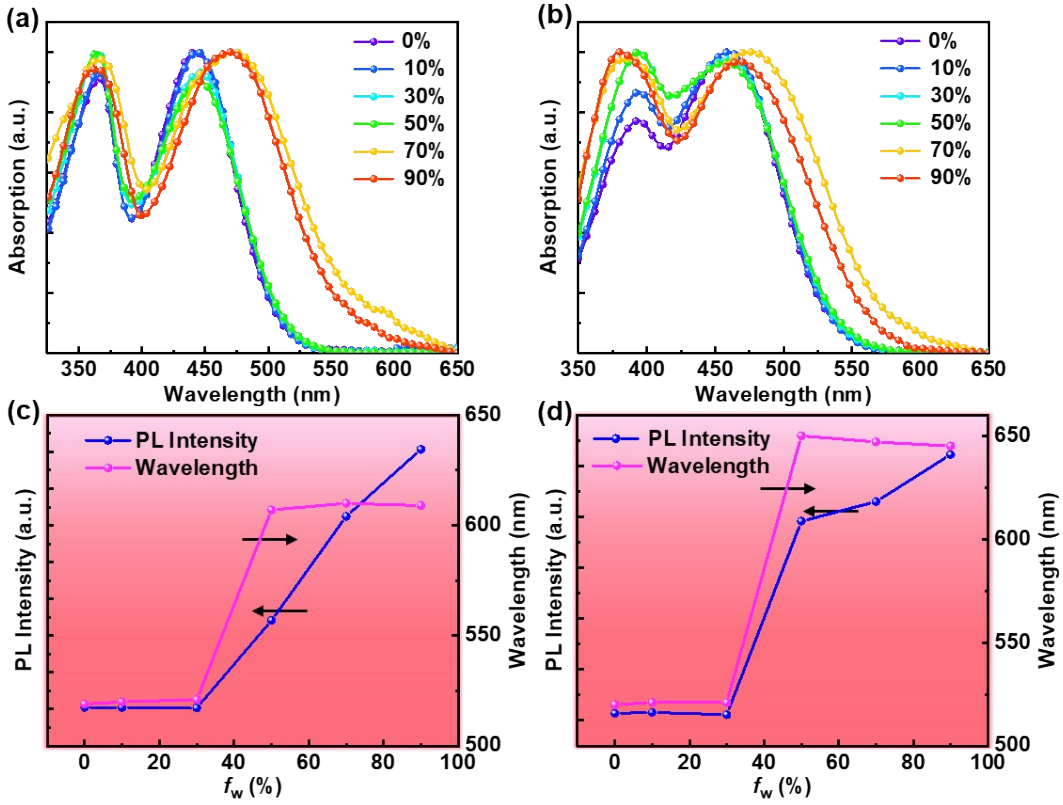

Fig. S4 UV-vis absorption spectra of (a) **BF_2-PhCz** and (b) **BF_2-PVCz** in DMSO/water mixtures with different water fractions (f_ws), the variation trend of PL intensity and wavelength with the elevated water fractions of (c) **BF_2-PhCz** and (d) **BF_2-PVCz**.

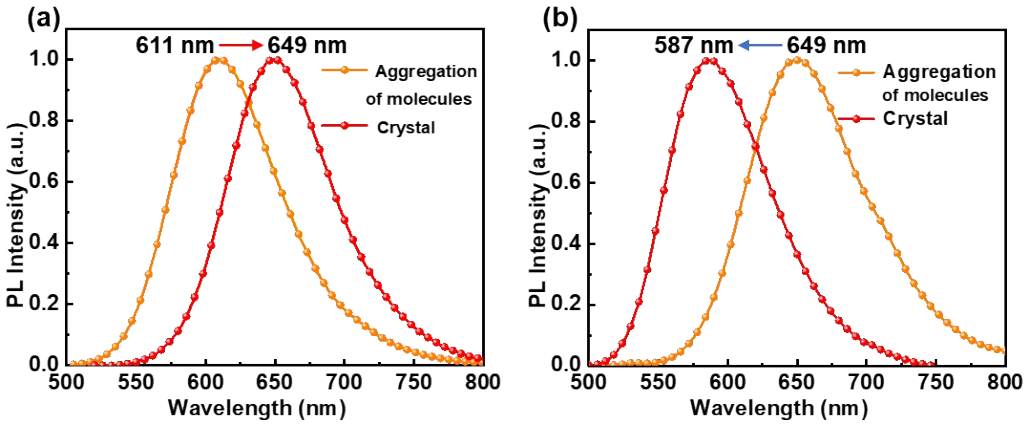

Fig. S5 The PL spectra of (a) **BF_2-PhCz** and (b) **BF_2-PVCz** in aggregation of molecules and crystal state.

4. Single Crystal Structure and Intermolecular Interactions Analysis

In Dimer **2**, the phenyl ring on the carbazole group was interacted with the boron atom on the boron difluoride of the adjacent molecule (B···H d_2 3.059 Å) to fix the bond angle and RIR of the phenyl ring. The moderate CH···π interactions between the phenyl ring and carbazole (d_3 2.792 Å) constrained molecular rotation and rigidified the molecular conformation (Fig. S6a). In addition, the CH···π interaction further enhanced the strength of F···H hydrogen bond, which would inhibit the dipole-dipole interactions and promote the blue shift with the increased intensity of emission.[S4] In Dimer **3**, the moderate F···H hydrogen-bond interactions between the phenyl ring and boron difluoride (d_4 2.638 Å) can also fix the bond angle and RIR of the phenyl ring (Fig. S6b). In Dimer **4**, CH···π interactions between the phenyl ring and carbazole (d_2 2.864 Å) also existed (Fig. S6c). These results indicated the presence of CH···π and F···H hydrogen-bond interactions in **BF_2-PVCz** crystal could effectively rigidify the molecular conformation, suppress the rotational and vibrational motions, which would conducive to weak the nonradiative decays.

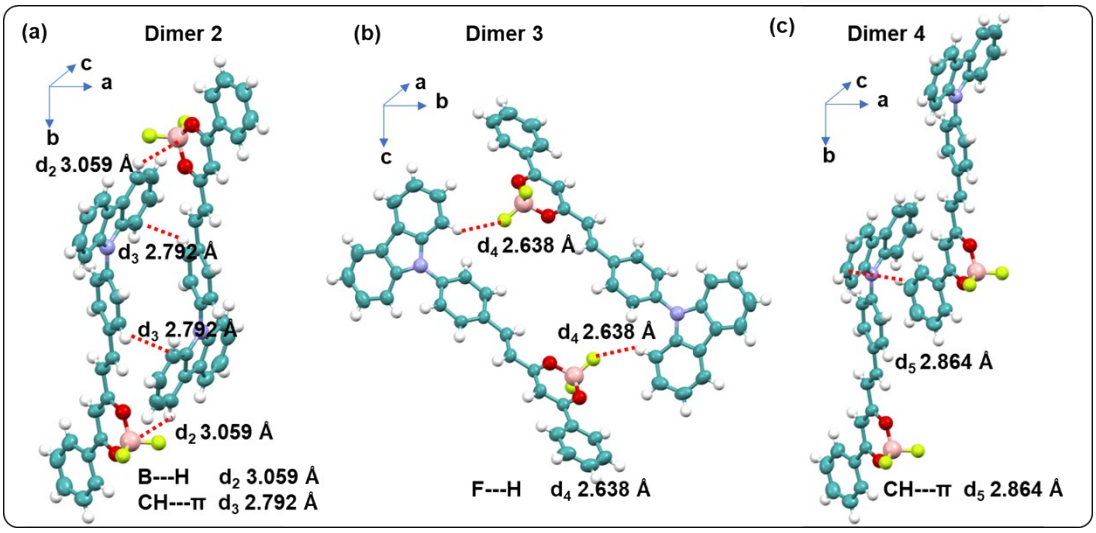

Fig. S6 Intermolecular interactions of (a) Dimer **2**, (b) Dimer **3**, and (c) Dimer **4** in the **BF_2-PVCz** single crystal.

On the three-dimensional Hirshfeld surface, the main interactions were the H···H interaction

(34.5%) and O···H interaction (2.74%), which could also be observed in the decomposed finger pattern (Fig. S7).

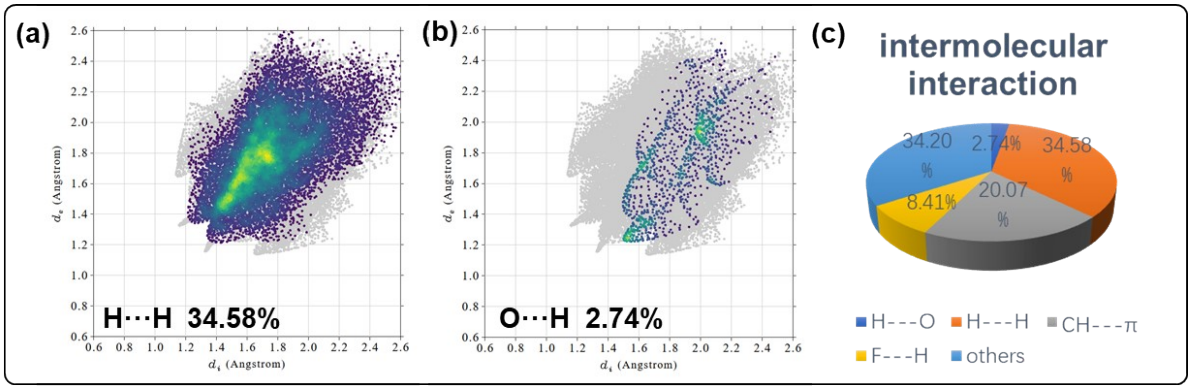

Fig. S7 (a) H···H weak interaction ratio fingerprint, (b) O···H weak interaction ratio fingerprint, (c) pie chart of proportion of each weak interaction for **BF_2-PVCz**.

Table S1 Crystal data and structure refinement for **BF_2-PVCz**

Compound	**BF_2-PVCz**
CCDC number	No. 2369031
Empirical formula	$C_{29}H_{20}BF_2NO_2$
Formula weight	463.27
Temperature/K	302.60(10)
Crystal system	triclinic
Space group	P-1
a/Å	8.9445(4)
b/Å	10.5005(5)
c/Å	14.2083(7)
α/°	99.936(4)
β/°	105.220(4)
γ/°	111.215(4)
Volume/Å^3	1146.08(10)
Z	2
ρ_{calc}g/cm^3	1.342
μ/mm^{-1}	0.094
F(000)	480.0
Crystal size/mm^3	0.11 × 0.07 × 0.04
Radiation	Mo Kα (λ = 0.71073)
2Θ range for data collection/°	4.358 to 61.922
Index ranges	-12 ≤ h ≤ 11, -14 ≤ k ≤ 14, -19 ≤ l ≤ 17
Reflections collected	16917
Independent reflections	5749 [R_{int}= 0.0284, R_{sigma}= 0.0375]
Data/restraints/parameters	5749/0/316
Goodness-of-fit on F^2	1.042
Final R indexes [I>=2σ (I)]	R_1= 0.0530, wR_2= 0.1337

Final R indexes [all data]	R_1= 0.0907, wR_2= 0.1512
Largest diff. peak/hole / e Å^{-3}	0.36/-0.41

5. MRL Properties

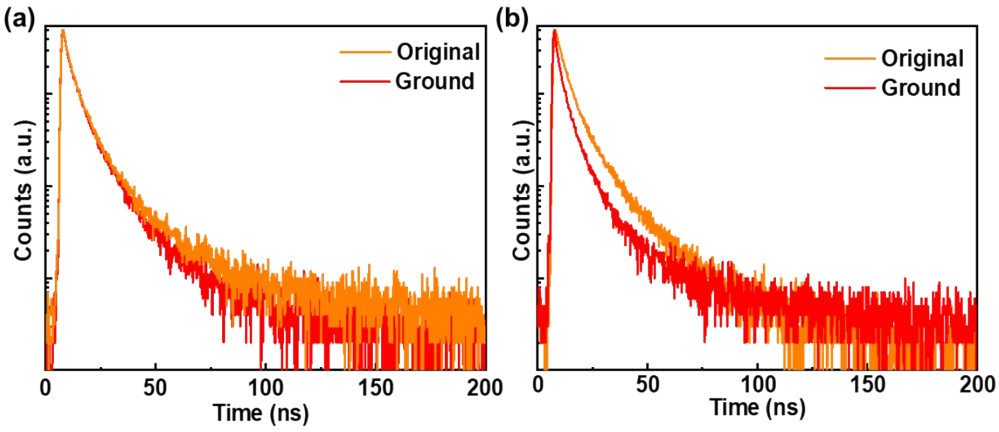

Fig. S8 Time-resolved fluorescence spectra of (a) **BF_2-PhCz** and (b) **BF_2-PVCz** (E_{ex}= 375 nm).

Table S2. Photophysical properties of **BF_2-PhCz** and **BF_2-PVCz** in the original and ground states

Compound	λ_O/λ_G (nm)	τ_O/τ_G (ns)	Φ_{FO}/Φ_{FG} (%)	k_{rO}/k_{rG} (ns^{-1})	k_{nrO}/k_{nrG} (ns^{-1})
BF_2-PhCz	649/647	9.13/7.92	15.34/13.00	0.017/0.016	0.107/0.110
BF_2-PVCz	587/641	8.16/6.81	26.76/6.00	0.033/0.0088	0.089/0.138

O: Original state, G: Ground state

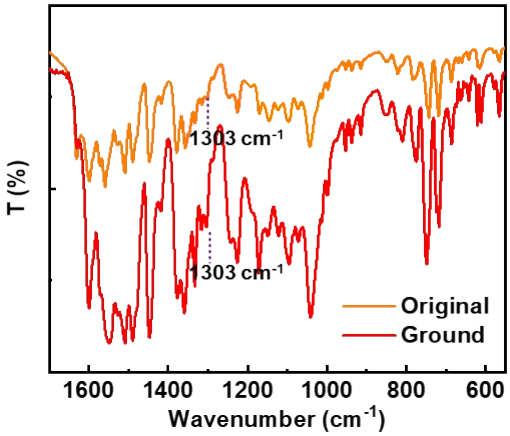

Fig. S9 FT-IR spectra of **BF_2-PhCz** before and after grinding

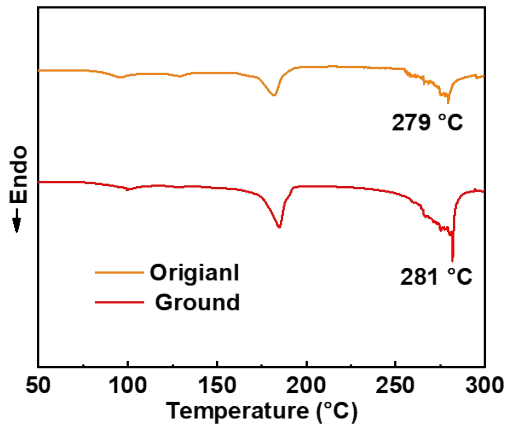

Fig. S10 The DSC curves of **BF_2-PhCz** in the original and ground states.

6. NMR spectra

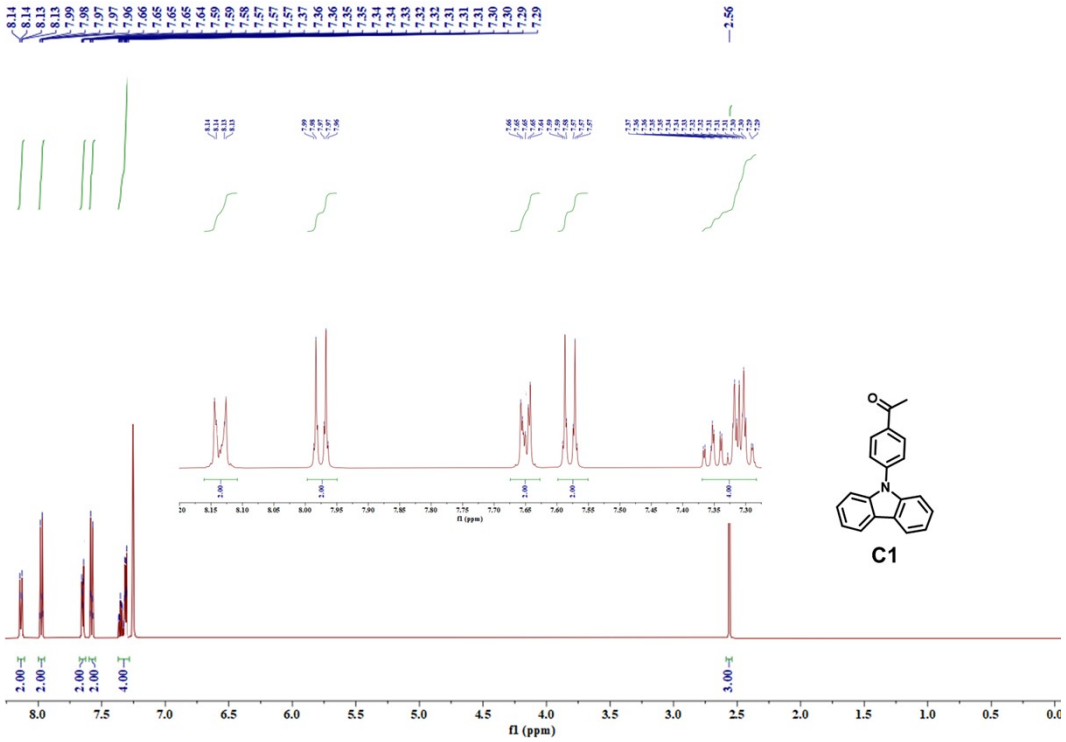

Fig. S11 ^{1}H NMR spectrum of $\mathbf{C_1}$.

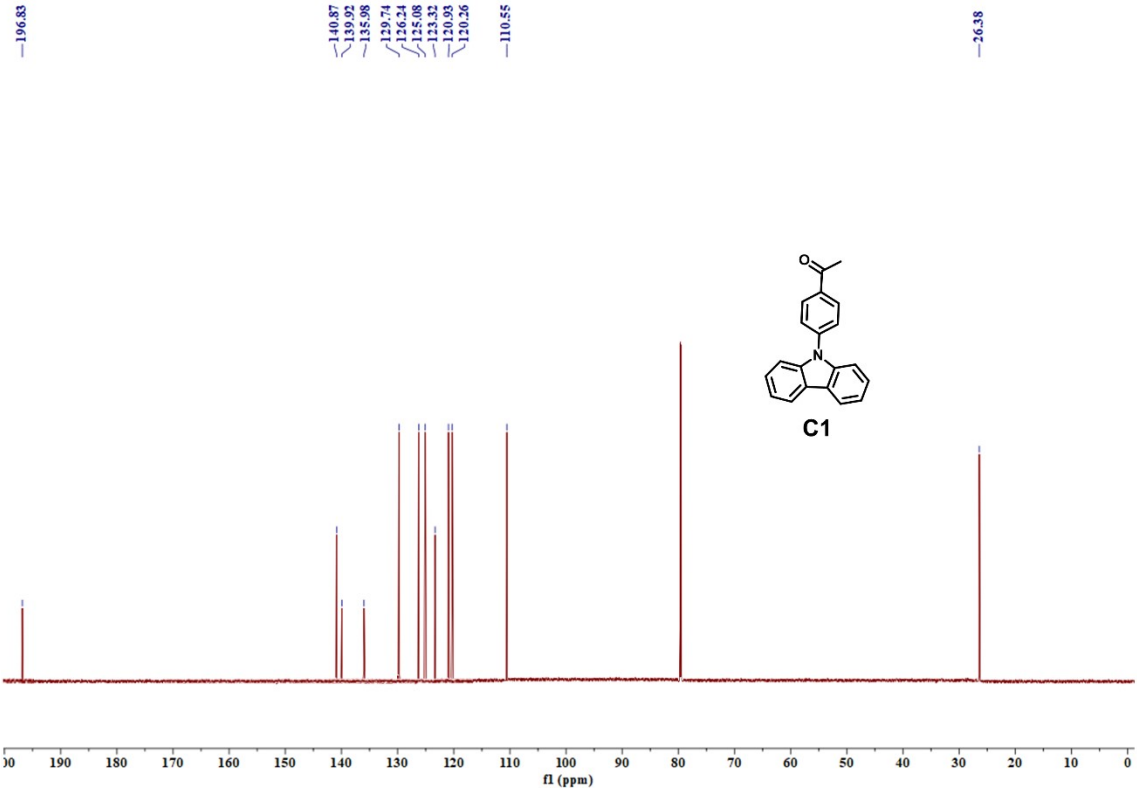

Fig. S12 ^{13}C NMR spectrum of $\mathbf{C_1}$.

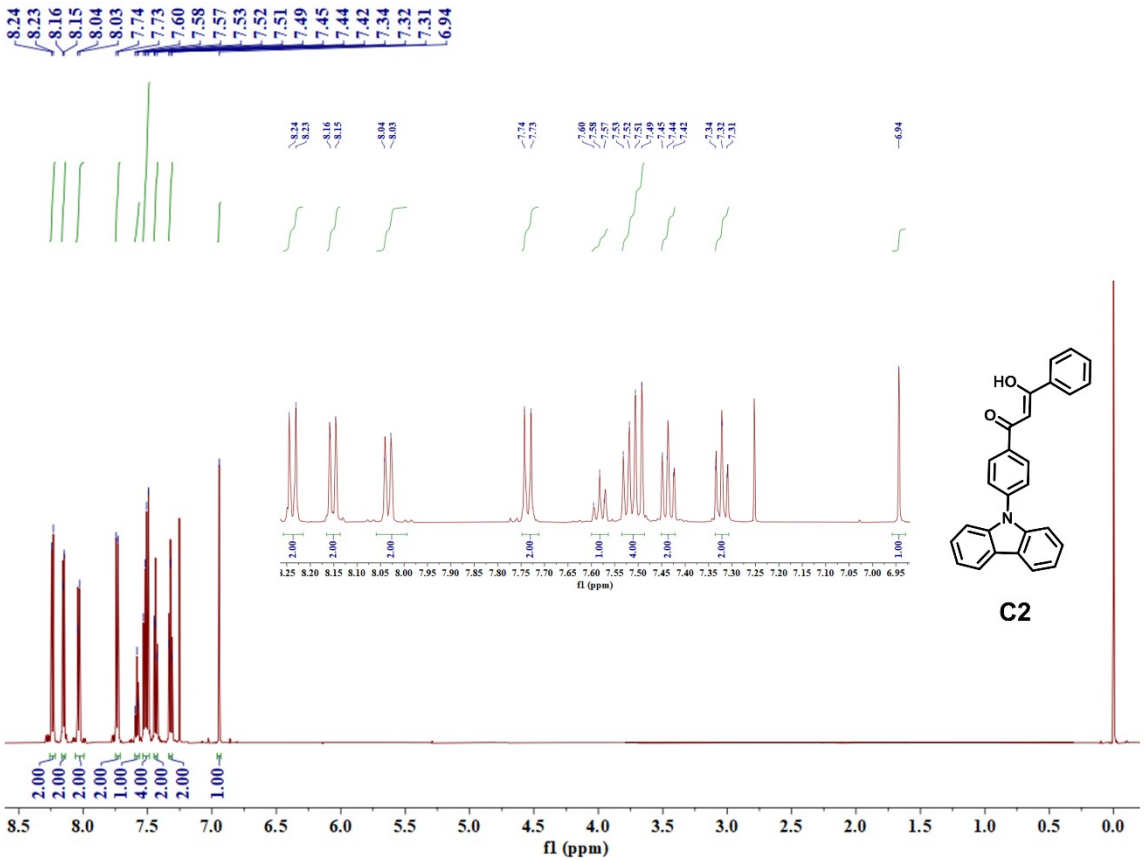

Fig. S13 ^{1}H NMR spectrum of $\mathbf{C_2}$.

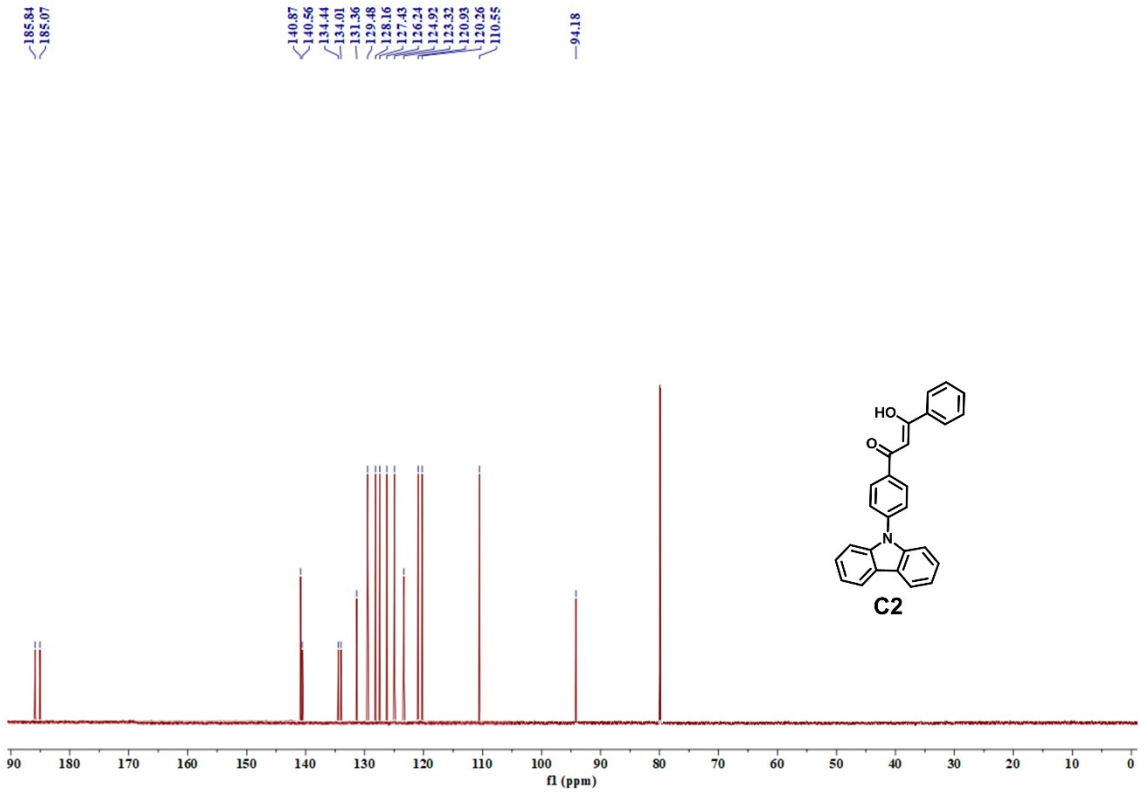

Fig. S14 ^{13}C NMR spectrum of $\mathbf{C_2}$.

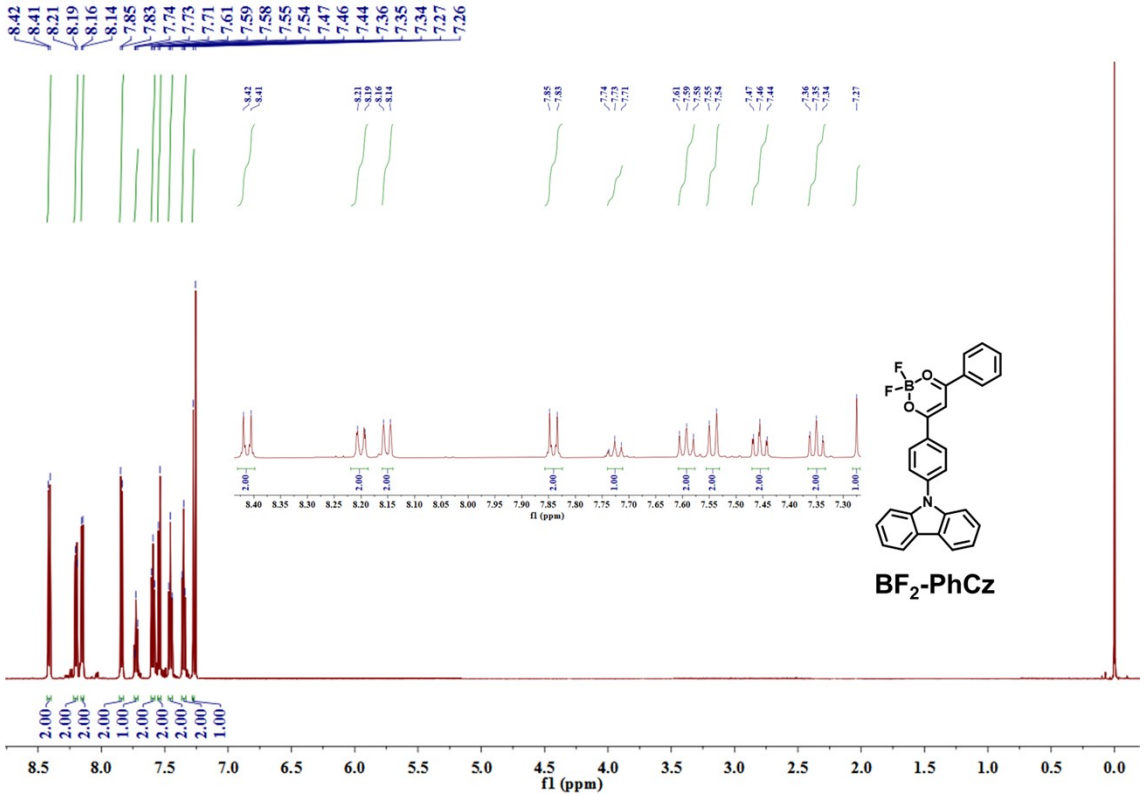

Fig. S15 ^{1}H NMR spectrum of **BF_2-PhCz**.

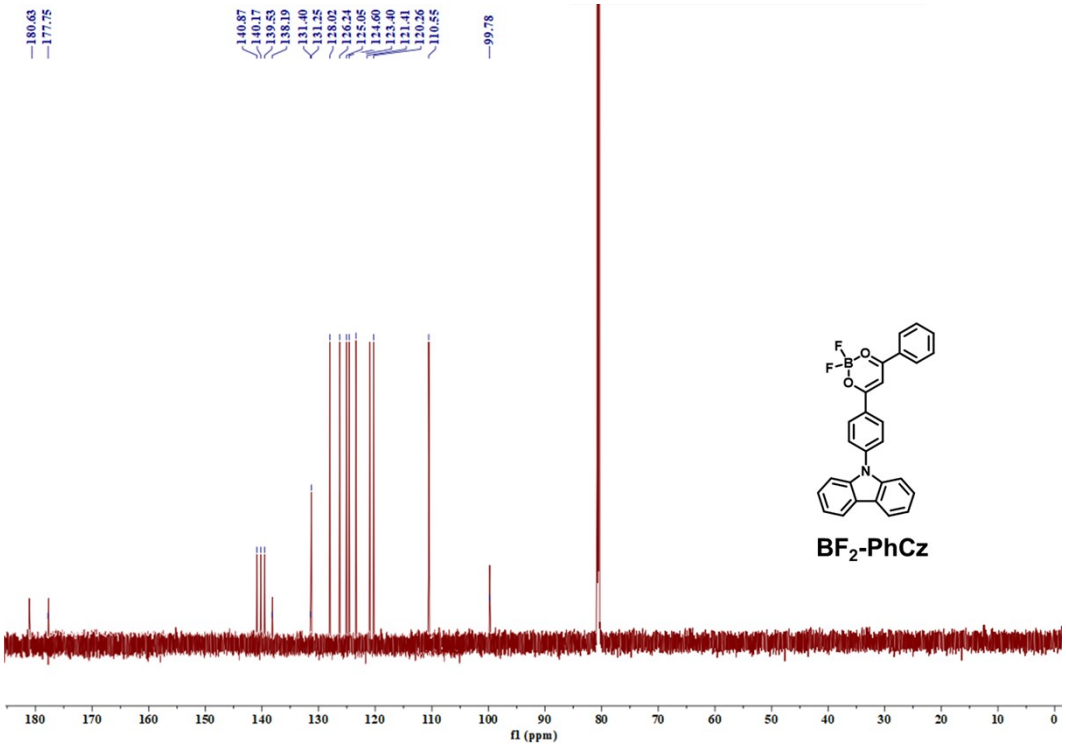

Fig. S16 ^{13}C NMR spectrum of **BF_2-PhCz**.

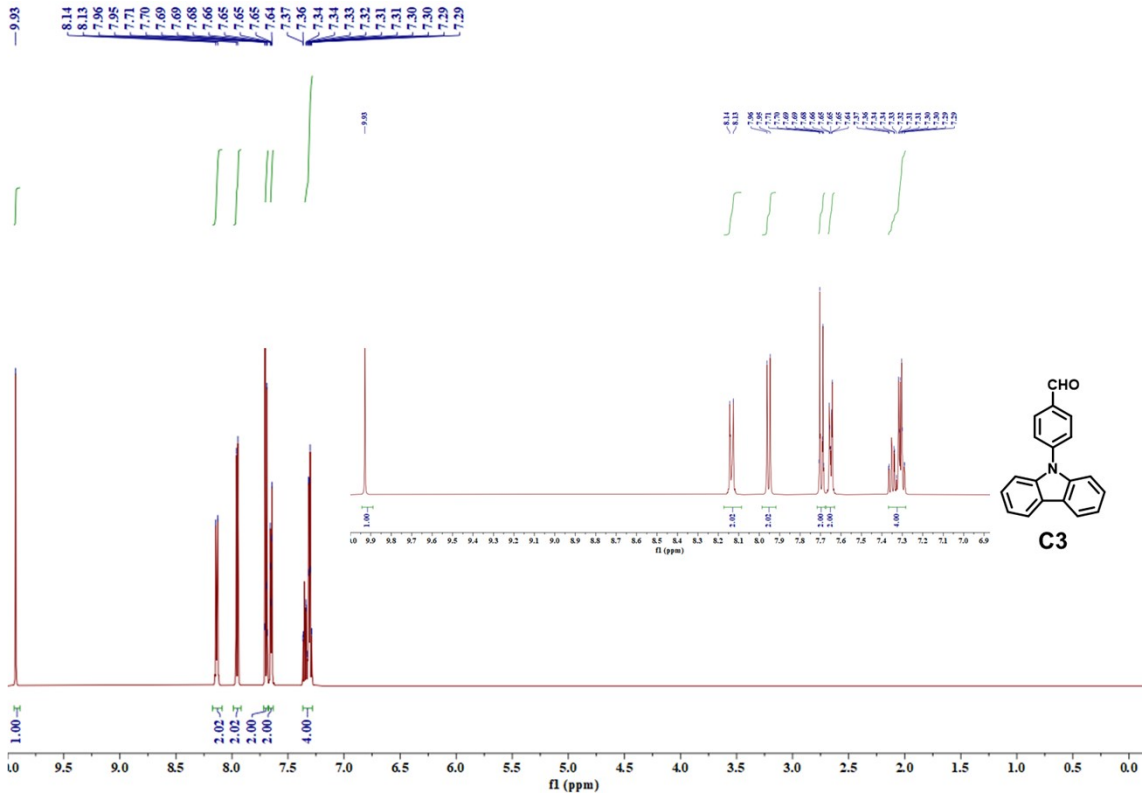

Fig. S17 ^{1}H NMR spectrum of **C$_3$**.

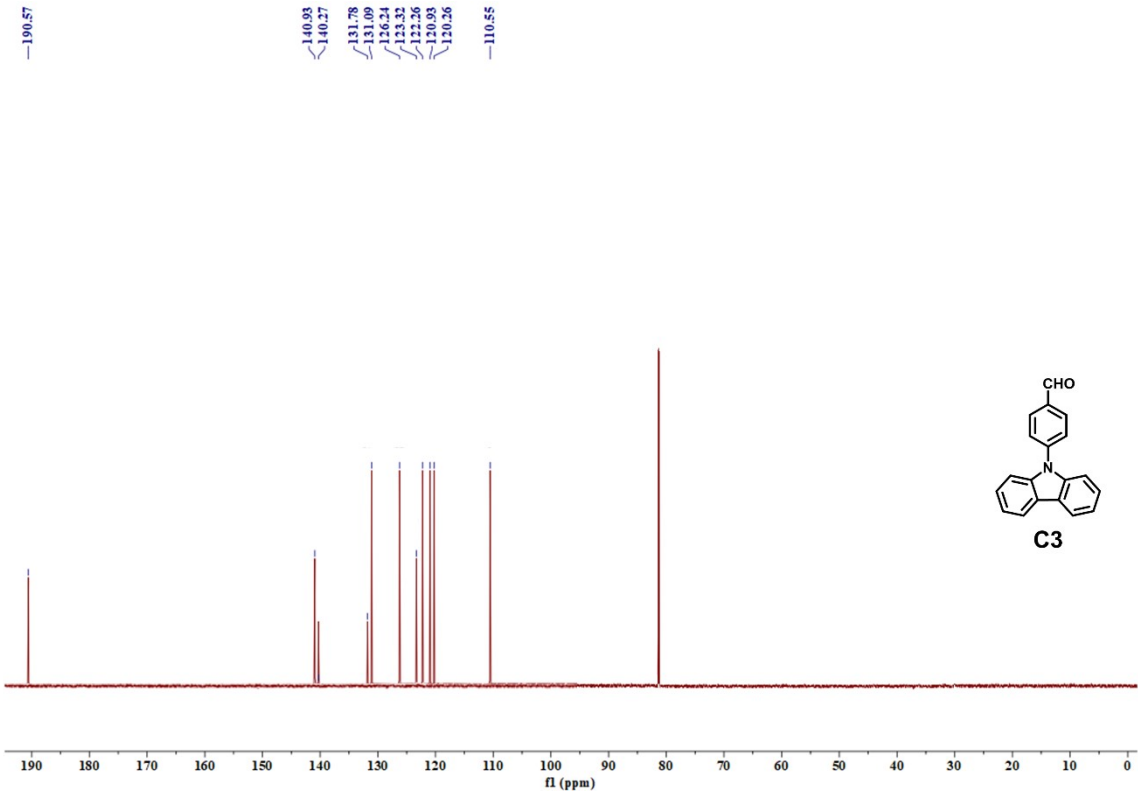

Fig. S18 ^{13}C NMR spectrum of **C$_3$**.

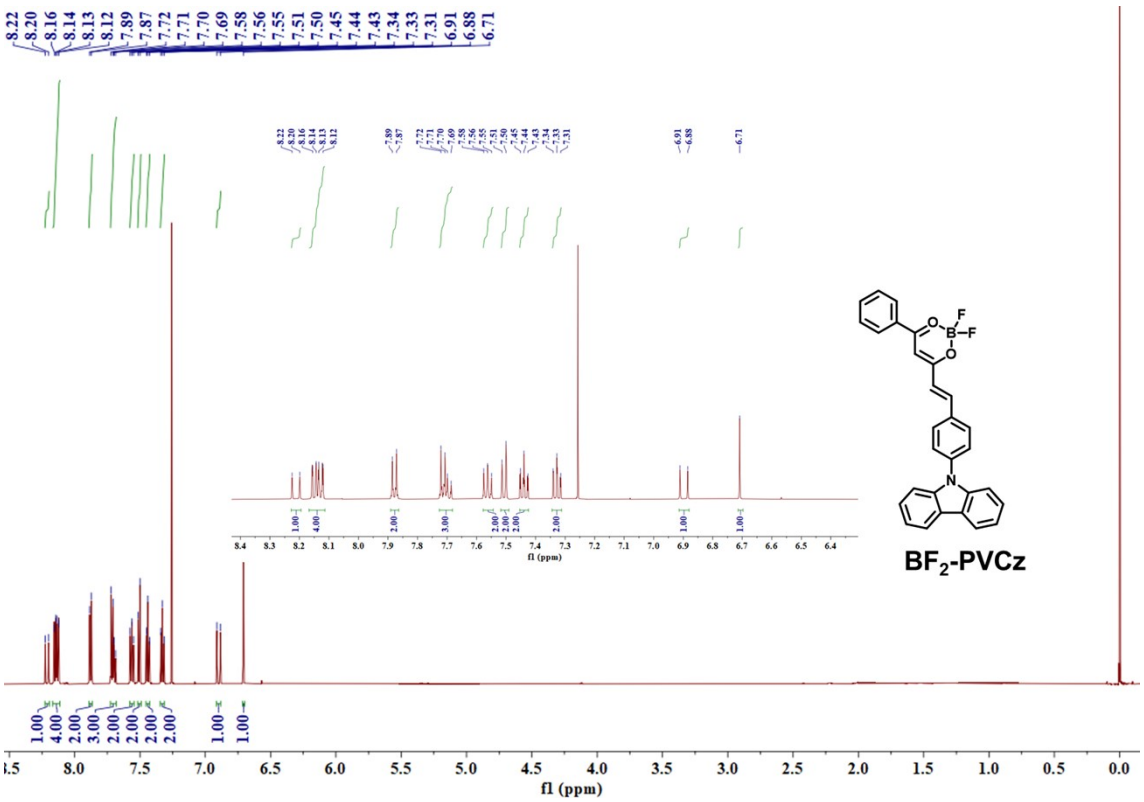

Fig. S19 ^{1}H NMR spectrum of **BF_2-PVCz**.

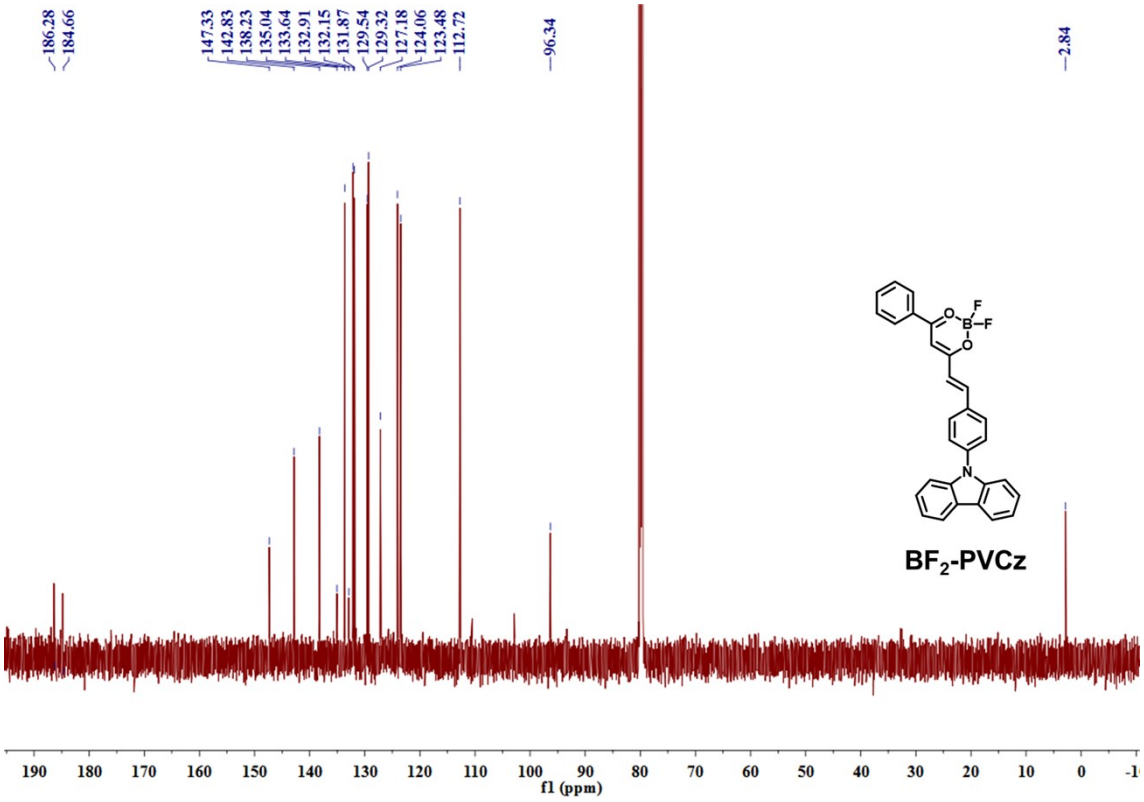

Fig. S20 ^{13}C NMR spectrum of **BF_2-PVCz**.

7. References

S1. T. Lu and F. Chen, *J. Comput. Chem.*, 2012, **33**, 580-592, DOI: 10.1002/jcc.22885.

S2. Z. Liu, T. Lu and Q. Chen, *Carbon*, 2020, **165**, 461-467, DOI: 10.1016/j.carbon.2020.05.023.

S3. W. Humphrey, A. Dalke and K. Schulten, *J. Mol. Graph.*, 1996, **14**, 33-38, DOI: 10.1016/0263-7855(96)00018-5.

S4. Z. Momeni and A. Ebrahimi, *Structural Chemistry,* 2016, **27**, 1199-1209, DOI: 10.1007/s11224-016-0745-6.